Civil Engineering Infrastructures Journal xx,xx
DOI: 10.22059/ceij.2026.399984.2359

A Robust Near-Optimal Sensor Placement Algorithm for Output-Only Structural Damage Detection with Uncertainties in Damages Scenarios

Sarparast Sadat, S. [1], Gholizad, A. [2,*]
[1] Ph.D. Candidate, Department of Civil Engineering, University of Mohaghegh Ardabili, Ardabil, Iran
[2] Professor, Department of Civil Engineering, University of Mohaghegh Ardabili, Ardabil, Iran
*Corresponding author E-mail: gholizad@uma.ac.ir

Received: 08/08/2025
Revised: 16/04/2026
Accepted: 22/06/2026

Abstract: The performance reliability of structural health monitoring methods depends on the accurate acquisition of a system's dynamic responses and the consideration of uncertainties related to optimal sensor placement. This study presents a two-step framework for Near-optimal sensor placement and evaluates its robustness especially against uncertainties arising from potential damage scenarios, and modeling noise. First, the identification of the system using Covariance-driven Stochastic Subspace Identification method in the form of a finite element model and in offline conditions is performed and healthy and damaged modes are extracted under assumed scenarios. A novel index based on modal strain energy changes is then introduced to guide sensor placement. The effectiveness of the proposed sensor configuration is subsequently validated using a genetic algorithm and benchmarked against the optimal configuration. Then, the accurate structural damage identification process is employed by applying the Reference-based Stochastic Subspace Identification method to the incomplete data obtained from the proposed sensor placement configuration and combining it with the Probabilistic Strategy to estimate the probability of damage in the structural members. The proposed framework effectively balances accuracy, resilience to uncertainty, and computational efficiency, offering a practical and scalable solution for reliable sensor deployment and damage detection in real-world structural systems.

Keywords: Structural Health Monitoring, Optimal Sensor Placement, Modal Strain Energy, Stochastic Subspace Identification, Damage Detection

1. Introduction

One of the primary objectives of structural health monitoring (SHM) processes is to identify potential damages within a structure. This area has been extensively studied and documented in numerous research articles and studies (Avci et al., 2021; Frigui et al., 2018; Gharehbaghi et al., 2022; Ghafouri et al., 2024). Among the methodologies employed in this field, operational modal analysis (OMA) methods are widely utilized to estimate system parameters and structural characteristics under operational or experimental conditions (Katam et al., 2023). A critical issue that has consistently been addressed in this context is the challenge of managing uncertainties, both in the structural response and in the accurate modeling of the system, as well as ensuring the reliability of the obtained results (Hou and Xia, 2021). However, certain OMA methods are capable of delivering structural parameters with acceptable accuracy, even in the presence of uncertainties (Magalhães et al., 2012; Ubertini et al., 2013; Foti et al., 2014; Rainieri and Fabbrocino, 2014; Brincker and Ventura, 2015). A fundamental requirement for system identification involves the installation of sensors at the degrees of freedom of the structure to extract and record its response. However, this approach is often constrained by limitations such as economic considerations and the specific characteristics of the structure. Addressing these challenges has led to the formulation of the optimal sensor placement (OSP) problem, which aims to determine a specific arrangement of a limited number of sensors to accurately identify the dynamic behavior of the system while minimizing errors (Ostachowicz et al., 2019; Barthorpe and Worden, 2020; Das and Saha, 2022; Rochuskis et al., 2022; Hassani and Dackermann, 2023). Under the conditions governing SHM methodologies, numerous optimization techniques and algorithms have been extensively explored in prior research. Among these, the Effective Independence Method (EFI) and the Modal Strain Energy (MSE) method have been widely investigated. Additionally, various optimization algorithms, such as the Genetic Algorithm (GA), have been employed, often utilizing objective functions like the Modal Assurance Criterion (MAC) (Rao and Anandakumar, 2008; Tong et al., 2014; Mendler et al., 2022; Yang. 2021). These approaches aim to enhance the efficiency and accuracy of SHM systems in evaluating structural integrity.

Within the domain of OMA techniques, the Stochastic Subspace Identification (SSI) method serves as a robust and effective signal processing approach for the identification of structural characteristics. This method utilizes recorded data to identify the system, enabling the determination of modal parameters for the entire structure. The computational robustness, superior performance, and high estimation accuracy of the SSI method have been consistently demonstrated and validated across numerous studies (Cascone et al., 2020; Ghosh et al., 2022; Liesecke et al., 2023). Peters and Roeck (2000) introduced the Reference-Based Stochastic Subspace Identification (Ref-SSI) method, building upon the foundational principles of the SSI technique. This approach assumes a limited number of sensors and utilizes the covariance of measured data to extract the modal parameters of a structure. These parameters are derived from the structure's response to ambient vibrations, enabling effective modal identification under operational conditions. In this method, the key concept is to deal with uncertainties arising from modeling the system and the response of the structure under consideration.

Due to the high sensitivity of mode shape vectors to damage occurrence and alterations in the stiffness matrix of a structure, the computation of changes in modal strain energy within structural members has been introduced as a reliable indicator for damage detection. This approach has been extensively utilized and validated in numerous studies (Behtani et al. 2020). Zhan and Yu (2014) introduced the Effective Independence-Improved Modal Strain Energy (EI-IMSE) method for optimal sensor placement in structural health monitoring. This approach integrates the Effective Independence (EI) and Improved Modal Strain Energy (IMSE) techniques to enhance the reliability and accuracy of the results. Muthuraman et al. (2016) utilized the MSE method to determine an initial sensor placement for the SHM process and potential damage detection. Furthermore, they applied a genetic algorithm to optimize the sensor placement pattern within the structure. In addition, they employed the Flexibility Matrix-Based Technique (FMBT) to accurately identify the precise location of structural damage. Arefi et al. (2020) introduced the Modified Mean Squared Error-Based Index (MMSEBI) to address the limitations of sensor placement across all degrees of freedom (DOF). The proposed method employs the Improved Reduction System (IRS) technique to reconstruct mode shapes. The efficacy of this approach was validated through the analysis of two numerical case studies and multiple damage patterns. Nguyen and Livaoğlu (2022) proposed a method that integrates MSE with updating techniques to detect and estimate damage severity in structures. Their approach ensures that the presence of noise does not compromise the accuracy of damage severity estimation. Through this process, damaged elements can be identified using mode shapes and updating techniques while considering various damage scenarios. Numerical validation results confirm the effectiveness of the proposed method. An et al. (2022) introduced a statistical algorithm for structural damage detection based on MSE, specifically designed for scenarios with limited data and ambient vibration measurements, where only operational mode shapes are available. This technique employs efficient algebraic equations to accurately identify damaged elements with varying degrees of damage within the structure. Additionally, it accounts for the presence of noise while simultaneously estimating both damage and modal factors. Kahouadji et al. (2023) proposed a hybrid method integrating a modified MSE index with robust optimization algorithms, utilizing finite element model simulations in MATLAB to identify structural damage. This approach enables precise localization of damage by incorporating a modified objective function within an optimization framework. While EI-IMSE and related MSE are defined in the selection process of sensors based on the magnitude of the effect on linear independence or / and modal strain energy coverage, our contribution combines (i) an MSE Change Ration (MSECR) that explicitly measures damage-induced redistribution of modal strain energy across many stochastic damage scenarios, with (ii) a Euclidean Impact-Index aggregation across scenarios (the Impact-Index) to identify elements most consistently sensitive to damage. This emphasis on change (healthy to damage) rather than only absolute MSE and the statistical sampling of damage scenarios distinguishes our Near-OSP approach.

Several studies have evaluated the use of Bayesian strategies during the damage identification stage to address the challenges posed by uncertainty in accurately detecting damaged elements, highlighting the effectiveness of this approach. Within this framework, the integration of results from various damage indices such as Damage indexes modal strain energy (DIMSE), frequency response function strain energy dissipation ratio (FRFSEDR), flexibility strain energy damage ratio (FSEDR), and residual force-based damage index (RFBDI) enables the precise and reliable identification of structural damage locations (Guo and Li, 2012; Barman et al., 2021; Mao et al., 2022).

In studies related to SHM, the optimal placement of sensors, the appropriate formulation of optimization problems, and the implementation of optimization algorithms face significant challenges due to uncertainties associated with the unknown location and severity of structural damage. As a result, employing a robust and near-optimal sensor placement strategy not only reduces the computational cost of optimization techniques but also supports the development of operational solutions for sensor deployment. It is important to note that the optimal sensor configuration for detecting one type of damage may differ from that required to detect another. Given the inherent uncertainty in the initial location and nature of damage, the sensor placement strategy must be robust against variations in potential failure scenarios, maintain near-optimal performance, and ensure sufficient stability for accurate damage identification. Traditional SHM methodologies often treat sensor placement and damage identification as separate tasks. Sensor placement techniques focus on maximizing information content without explicitly considering damage sensitivity. In contrast, damage detection methods typically assume that sensors are already optimally placed, which may not be the case in practice. Without incorporating damage sensitivity into the placement strategy, sensors may be located in areas that are less responsive to damage, potentially leading to missed detections or false alarms. A hybrid framework can address this gap by ensuring sensors are strategically placed in locations that are near-optimal for damage identification, thereby improving the accuracy and reliability of SHM systems. The MSE index, which has a clear physical interpretation and is highly sensitive to local and minor stiffness changes, supports practical applications in SHM. To compute this index under operational conditions, the SSI method can be employed, as it is well-suited for real-world scenarios. SSI is robust against measurement noise and enables reliable estimation of modal parameters, thereby enhancing the accuracy of system identification. This research bridges the gap between sensor placement and damage detection by ensuring that sensors are positioned in locations near-optimized for accurate damage identification. To meet these needs, an index is introduced to support the development of a robust sensor placement strategy, significantly improving the efficiency and reliability of the damage detection process. A key advantage of this approach is that it eliminates the need for repetitive calculations in determining the optimal sensor layout. Following finite element modeling and dynamic analysis of the structure, variations in the modal strain energy of structural elements are integrated into a probabilistic framework to enable effective monitoring and damage identification. This paper aims to address the aforementioned challenges through a two-step approach. In the first step, while introducing the flowchart of the proposed near-optimal sensor placement strategy, its performance is evaluated in comparison with a traditional sensor placement optimization problem in the SHM framework. In the second step, a hybrid approach is employed in the form of using a Bayesian strategy to improve the accuracy of damage detection based on the proposed index. We propose a mode likelihood mapping from MSECR to mode-specific damage likelihood and a simple independence fusion across modes (product rule) with a uniform prior. Our approach is based on using MSECR as the per-mode evidence function,(ii) combining Ref-SSI estimated mode information with the offline Impact-Index /Near-OSP, and (iii) quantifying repeatability via Monte-Carlo SNR experiments (N=50 per SNR).

2. Method

2.1. STEP 1: Flowchart of a Near-OSP Pattern

In addressing the OSP problem, a structure can be evaluated under multiple potential failure scenarios. As a result, the optimal sensor configuration may vary depending on the specific damage scenario. Furthermore, considering the inherent challenges of SHM and the uncertainties regarding the location and severity of damage, developing an OSP model that accounts for these uncertainties can significantly enhance efficiency. Based on the background of the present research, changes in MSE can be utilized to determine optimal sensor placement within a limited number of DOF of the structure. Accordingly, the proposed sensor locations are identified using an index calculated by extracting the mode shapes of the structure and analyzing the differences in MSE between damaged and undamaged structural elements. In the proposed framework, MSE for the healthy structure is determined by solving the eigenvalue problem through finite element modal analysis. For the damaged structure, system identification is performed in offline conditions by modeling the finite element model and considering all the necessary assumptions for the use of SSI - COV method. It is assumed that each structural element may experience damage independently, modeled as a reduction in its elastic modulus each representing a distinct damage scenario. Using the proposed Modal Strain Energy Change Ratio (MSECR), nodes connected to elements exhibiting the highest MSE variation are identified as near-optimal locations for sensor placement.

2.1.1. System Identification under Complete Data

This section introduces the dynamic system and its state-space representation, which form the foundation of the SSI-COV method. The focus is on output-only modal identification, where the system's modal parameters such as natural frequencies, damping ratios, and mode shapes are estimated solely from the response data. Within this approach, uncertainties such as measurement noise and modeling inaccuracy are systematically considered, and statistical principles are used to analyze the recorded structural response data, which allows for accurate system characterization. The behavior of a discrete mechanical system consisting of n_2 masses connected by dampers and springs is described by a second-order linear differential equation with constant coefficients as follows (Peeters and Roeck, 2000; Ewins, 2009):

$$M\ddot{U}(t) + C_2\dot{U}(t) + KU(t) = F(t) = B_2u(t) \tag{1}$$

Where *M, C* and $K \in \mathbb{R}^{n_2 \times n_2}$ represents the mass, damping and stiffness matrices, respectively. $F(t) \in \mathbb{R}^{n_2 \times 1}$ is equivalent to the excitation force and $U(t) \in \mathbb{R}^{n_2 \times 1}$ is the displacement vector at continuous time *t*. The force vector $F(t)$ is factorised into a matrix $B_2 \in \mathbb{R}^{n_2 \times m}$ describing the inputs in space and a vector $u(t) \in \mathbb{R}^{m \times 1}$ describing the *m* inputs in time. Assuming unknown noise sources along with the applied force *F*, which may lead to incomplete knowledge of the applied excitation, using control theory and the appropriate form of the continuous-time state-space, Eq. (1) can be formulated as follows (Juang, 1994):

$$\dot{x}(t) = A_cx(t) + B_cu(t), \tag{2}$$

$$x(t) = \begin{bmatrix} U(t) \\ \dot{U}(t) \end{bmatrix}, A_c = \begin{bmatrix} 0 & I_{n_2} \\ -M^{-1}K & -M^{-1}C_2 \end{bmatrix}, B_c = \begin{bmatrix} 0 \\ M^{-1}B_2 \end{bmatrix} \tag{3}$$

Where $A_c \in \mathbb{R}^{n \times n}$ is the state matrix of the system with dimensions ($n = 2n_2$), $B_c \in \mathbb{R}^{n \times m}$ is the input matrix, and $x(t) \in \mathbb{R}^{n \times 1}$ equivalent of the state vector, which can be defined to encompass *n* states. Given that acceleration, velocity and displacement can be effectively monitored using *l* sensors into the system, the following equation can be presented:

$$y(t) = C_a\ddot{U}(t) + C_v\dot{U}(t) + C_dU(t) \tag{4}$$

Where $y(t) \in \mathbb{R}^{l \times 1}$ represents the system output and $C_a, C_v, C_d \in \mathbb{R}^{l \times n_2}$ denotes the output matrices for acceleration, velocity, and displacement. These matrices can be defined as Eq. (5) and convert Eq. (4) into the following expression:

$$C_c = [C_d - C_a M^{-1} K \quad C_v - C_a M^{-1} C_2] \ , D_c = C_a M^{-1} B_2 \tag{5}$$

$$y(t) = C_c x(t) + D_c u(t) \tag{6}$$

Where $C_c \in \mathbb{R}^{l\times n}$ represents the output matrix and $D_c \in \mathbb{R}^{l\times m}$ will be defined as the direct transfer matrix. These equations are presented as a continuous-time state-space model, implying that the system can be evaluated at any time $t \in \mathbb{R}$. However, it's important to note that sampling is performed discretely at time intervals k∈ℕ, kΔt. Consequently, both time samples and noise will impact on the acquired data. Considering the concepts of eigenvalues, the Jordan form of the matrix, and the relationships related to Taylor series, the discrete form of the state, input, output, and direct transfer matrices is expressed as follows (Chen, 1984):

$$A = e^{A_c T}, B = \left(\int_0^T e^{A_c \tau} d\tau\right) B_c, C = C_c, D = D_c \tag{7}$$

Considering the noises, the response value and state vector can be written in the following form (Juang, 1994):

$$\begin{gathered} x_{k+1} = A x_k + B u_k = A x_k + B u_k + \omega_k \\ y_k = C x_k + D u_k = C x_k + D u_k + \upsilon_k \end{gathered} \tag{8}$$

$x_k = x(kT) = x(K\Delta t)$ represents the discrete time state vector, $w_k \in \mathbb{R}^{n\times 1}$ is the uncertainty noise vector in modeling and $\upsilon_k \in \mathbb{R}^{l\times 1}$ is the uncertainty noise vector in measurement. Both of these noise vectors are unmeasurable. However, if it is assumed that these noises correspond to a white noise pattern with zero mean and follow the Gaussian distribution and are independent of each other, the covariance matrix of these uncertainties can be expressed as follows:

$$E\left[\begin{pmatrix} \omega_k \\ \upsilon_p \end{pmatrix} \begin{pmatrix} \omega_q^T \upsilon_q^T \end{pmatrix}\right] = \begin{pmatrix} Q & S \\ S^T & R \end{pmatrix} \delta_{pq} \tag{9}$$

Where E represents the Expected Value, δ_{pq} is Kroniker delta and $R \in \mathbb{R}^{l\times l}$, $S \in \mathbb{R}^{n\times l}$ are the covariance matrices of uncertainty noise vectors. In experimental problems, the input u_k disappears from Eq. (8) because this value is shown in the form of noise. Therefore, for the discrete stochastic state space model, the equations can be presented in the following form:

$$\begin{gathered} x_{k+1} = A x_k + \omega_k \\ y_k = C x_k + \upsilon_k \end{gathered} \tag{10}$$

Noises with zero mean ($E[\upsilon_k] = E[w_k] = 0$) and the stochastic process in the form of stationary with zero mean ($E[x_k x_k^T] = \Sigma, E[x_k] = 0$) is assumed that the covariance matrix is independent of time k. w_k, υ_k as the noises involved in the problem will be independent of the state $E[x_k \upsilon_k^T] = E[x_k w_k^T] = 0$, therefore the output covariance variable matrix Λ_i and the next state-output covariance matrix G is provided as:

$$\Lambda_i \equiv E[y_{k+i} y_k^T] \in \mathbb{R}^{l\times l} \tag{11}$$

$$G \equiv E[x_{k+1} y_k^T] \in \mathbb{R}^{n\times l} \tag{12}$$

According to the above definitions, the following properties can be deduced for the stated equations (Peeters and Roeck, 2000):

$$\Lambda_0 = C\Sigma C^T + R, \qquad \Sigma = A\Sigma A^T + Q \tag{13}$$

$$\Lambda_i = CA^{i-1}G, \qquad G = A\Sigma C^T + S \tag{14}$$

In the following, all the measured values are collected in a matrix called the Henkel matrix, which has $2i$ blocks and j columns. The first i block has r rows and the next i block has l rows that are scaled by a factor $1/\sqrt{j}$ to match the definition of covariance according to Eq. (11). The correctness of this relationship is guaranteed when the data is ergodic and contains infinite information. If any of these conditions are not satisfied, the mentioned relationship will not be equal to the covariance of the outputs, but it is only an estimate of it: (15)

$$H \equiv \frac{1}{\sqrt{j}} \left[\begin{array}{cccc} y_0 & y_1 & \cdots & y_{j-1} \\ y_1 & y_2 & \cdots & y_j \\ \cdots & \cdots & \cdots & \cdots \\ y_{i-1} & y_i & \cdots & y_{i+j-2} \\ \hline y_i & y_{i+1} & \cdots & y_{i+j-1} \\ y_{i+1} & y_{i+2} & \cdots & y_{i+j} \\ \cdots & \cdots & \cdots & \cdots \\ y_{2i-1} & y_{2i} & \cdots & y_{2i+j-2} \end{array} \right] \equiv \left(\frac{Y_{0|i-1}}{Y_{i|2i-1}} \right) \equiv \left(\frac{Y_p}{Y_f} \right) \frac{\text{"past"}}{\text{"future"}} \tag{15}$$

The observability matrix and the controllability matrix can also be expressed as follows, where the rank of the observability matrix will be equal to n:

$$O_i = \begin{pmatrix} C \\ CA \\ CA^2 \\ \cdots \\ CA^{i-1} \end{pmatrix} \in \mathbb{R}^{li\times n} \tag{16}$$

$$C_i \equiv \left(A^{i-1}G \;\; A^{i-2}G \;\; \cdots \;\; AG \;\; G \right) \in \mathbb{R}^{n\times ri} \tag{17}$$

The results of the covariance function of the output data are collected in Toeplitz matrix. This matrix is a constant diameter matrix, that each sub-diameter from left to right has a constant value:

$$T_{l|i} = \begin{pmatrix} \Lambda_i & \Lambda_{i-1} & \cdots & \Lambda_1 \\ \Lambda_{i+1} & \Lambda_i & \cdots & \Lambda_2 \\ \cdots & \cdots & \cdots & \cdots \\ \Lambda_{2i-1} & \Lambda_{2i-2} & \cdots & \Lambda_i \end{pmatrix} \tag{18}$$

Using Eq. (15), the Toeplitz matrix can be rewritten in the following form:

$$T_{1|i} = Y_f Y_p^T \tag{19}$$

Considering Eq. (14) and using the Singular Value Decomposition (SVD) method on the Toeplitz matrix, the decomposed form of this matrix can be presented as follows:

$$T_{1|i} = Y_f Y_p^T = \begin{pmatrix} C \\ CA \\ \cdots \\ CA^{i-1} \end{pmatrix} \begin{pmatrix} A^{i-1} & \cdots & AG & G \end{pmatrix} = O_i C_i \tag{20}$$

$$T_{1|i} = USV^T = \begin{pmatrix} U_1 & U_2 \end{pmatrix} \begin{pmatrix} S_1 & 0 \\ 0 & 0 \end{pmatrix} \begin{pmatrix} V_1^T \\ V_2^T \end{pmatrix} = U_1 S_2 V_1^T \tag{21}$$

Where $U \in \mathbb{R}^{li \times li}$ and $V \in \mathbb{R}^{ri \times ri}$ are orthogonal matrices ($U^T U = UU^T = I_{li}, V^T V = VV^T = I_{ri}$) and $S \in \mathbb{R}^{li \times ri}$ is a diagonal matrix that will present singular values in descending order. Next, by equating Eqs. (20) and (21) can write:

$$O_i = U_1 S_1^{\frac{1}{2}}, C_i = S_1^{\frac{1}{2}} V_1^T. \tag{22}$$

By using Eqs. (16) and (17), C is equal to the first l-row block of the observability matrix O_i and G is equal to the last r column block of the controllability matrix C_i. Therefore, the state matrix A can be obtained by decomposing the new Toeplitz matrix with a shifted block as follows:

$$T_{2|i+1} = O_i A C_i \tag{23}$$

By solving Eq. (23) and considering Eq. (22), the state matrix can be rewritten in the following form:

$$A = O_i^{\dagger} T_{2|i+1} C_i^{\dagger} = S_i^{-\frac{1}{2}} U_1^T T_{2|i+1} V_1 S_i^{-\frac{1}{2}} \tag{24}$$

The symbol $(\blacksquare)^{\dagger}$ represents the pseudo-inverse of the matrix. The dynamic behavior of the system is completely characterized by its eigenvalues:

$$A = \Psi \Lambda \Psi^{-1} \tag{25}$$

Where $\Lambda = diag(\lambda_q) \in \mathbb{C}^{n \times n}$, $q = 1, \ldots, n$ is a diagonal matrix containing the discrete-time complex eigenvalues and $\Psi \in \mathbb{C}^{n \times n}$ contains eigenvectors. The equation of the continuous time state is equivalent to the equation of the second-order matrix of motion and as a result, the eigenvalues and eigenvectors will be the same and can be obtained by an eigenvalue decomposition of the continuous-time state matrix:

$$A_c = \Psi_c \Lambda_c \Psi_c^{-1} \tag{26}$$

Where $\Lambda_c = diag(\lambda_{cq}) \in \mathbb{C}^{n \times n}$ is a diagonal matrix containing the continuous-time complex eigenvalues and $\Psi_c \in \mathbb{C}^{n \times n}$ contains eigenvectors. According to Eq. (8):

$$A = \exp(\Lambda_c \Delta t), \Psi_c = \Psi, \lambda_{c_q} = ln(\lambda_q)/\Delta t \tag{27}$$

The eigenvalues of A_c occur in complex conjugated pairs and can be written as:

$$\lambda_{c_q}, \lambda_{c_q}^* = -\xi_q \omega_q \pm j\omega_q \sqrt{1 - \xi_q^2} \tag{28}$$

Where ξ_q is the modal damping ratio and ω_q is the eigenfrequency of mode q (rad/s). The mode shapes $\Phi_q \in \mathbb{C}^{l\times n}$ at the sensor location are the observed parts of the system eigenvectors and can be written:

$$\Phi_q = C\,\Psi_q \tag{29}$$

Therefore, the modal parameters of the system are obtained through the *A* and *C* matrices.

2.1.2. Modal Analysis

The purpose of this section is to provide a theoretical foundation for understanding how modal parameters specifically natural frequencies and mode shapes are derived from the system's mass and stiffness matrices. This is particularly relevant to the finite element model (FEM) used in the sensor placement stage, where undamped systems are often assumed for simplicity. Modal analysis is a fundamental technique for investigating the dynamic behavior of linear systems. It involves extracting the system's natural frequencies and mode shapes, which are obtained from the equation of motion as follows (Arefi et al. 2020, Teimouri et al. 2021, Nguyen and Livaoğlu 2022, Khatir et al. 2019):

$$M\ddot{u} + K\dot{u} = 0 \tag{29}$$

Where *M* represents the mass matrix of the structure, *u* denotes the vector containing nodal displacements and *K* signifies the stiffness matrix of the healthy structure. Natural frequencies and mode shapes are obtained by solving the eigenvalue problem:

$$([K] - \omega_i^2[M])\{\Phi\} = 0, \qquad i = 1,2,\dots,nDOF \tag{31}$$

Where ω represents the frequency, Φ equivalent to the mode shape matrix and *nDOF* corresponds to the number of degrees of freedom in the healthy structure.

2.1.3. Proposed Index of Near-OSP

The modal strain energy matrix of the healthy and damaged structure will be equal to:

$$MSE_{ij}^{u} = \Phi_i^T K_j \Phi_i, i = 1,2,\dots,m, j = 1,2,\dots,n \tag{32}$$

$$MSE_{(ssi-cov)ij}^{d} = \Phi_{(ssi-cov)i}^{d^T} K_j \Phi_{(ssi-cov)i}^{d}, i = 1,2,\dots,m, j = 1,2,\dots,n \tag{33}$$

Here, K_j represents the stiffness matrix of the *j*th element, and Φ_i denotes the mode shape vector corresponding to the *i*th mode of the structure. To apply the SSI-COV method, it is assumed that sensors are installed at all degrees of freedom of the structure. Accordingly, the modal strain energy of the *j*th element both for the healthy and damaged states of the structure under the *d*th failure scenario (d = 1, 2,…,s ; s = number of element structure) is calculated using the following expression (Sarparast.S and Gholizad, 2026):

$$MSE_j^u = \sum_{i=1}^{m} \Phi_i^T K_j \Phi_i \tag{34}$$

$$MSE^d_{(ssi-cov)j} = \sum_{i=1}^{m} \Phi^{d^T}_{(ssi-cov)i} K_j \Phi^d_{(ssi-cov)i} \tag{35}$$

To calculate the modal strain energy of the entire structure with *n* elements in the *i*th mode, the following expression can be used:

$$MSE^u_i = \sum_{j=1}^{n} MSE^u_{ij} \tag{36}$$

$$MSE^d_{(ssi-cov)i} = \sum_{j=1}^{n} MSE^d_{(ssi-cov)ij} \tag{37}$$

The normalized modal strain energy of element *j* in both healthy and damaged structures in the "ith" mode can be expressed as follows:

$$NMSE^u_{ij} = \frac{MSE^u_{ij}}{MSE^u_i}, j = 1,\ldots,n \tag{38}$$

$$NMSE^d_{(ssi-cov)ij} = \frac{MSE^d_{(ssi-cov)ij}}{MSE^d_{(ssi-cov)i}}, j = 1,\ldots,n \tag{39}$$

Therefore, the modal strain energy change ratio (MSECR) index of member *j* in mode *i* for failure scenario *d* is presented in the form of the following equation, where the zero value corresponds to the healthy member and the non-zero value corresponds to the unhealthy member:

$$MSECR^d_{(ssi-cov)ij} = max\left(0, \frac{NMSE^d_{(ssi-cov)ij} - NMSE^u_{ij}}{NMSE^u_{ij}}\right) \tag{40}$$

The index described with the assumption of the first *nm* modes of the structure response is presented as follows:

$$MSECR^d_{(ssi-cov)j} = max\left(0, \frac{\sum_{i=1}^{nm} NMSE^d_{(ssi-cov)ij} - \sum_{i=1}^{nm} NMSE^u_{ij}}{\sum_{i=1}^{nm} NMSE^u_{ij}}\right) \tag{41}$$

It is noted that the normalization in Eqs. (38)–(39) is performed to remove global scaling effects associated with stiffness degradation and to emphasize the relative redistribution of modal strain energy among structural elements. While both the numerator and denominator in Eq. (39) vary under damage, damage detectability is ensured through the subsequent Modal Strain Energy Change Ratio (MSECR), which explicitly compares the damaged and healthy normalized energy distributions. Inter-scenario comparability is achieved at the MSECR and impact index levels, rather than at the normalized MSE stage. If all potential failure scenarios (equivalent to the total number of structural members and individually) are considered, the cumulative index of modal strain energy changes for each member can be quantified using a novely defined metric referred to as the impact index, expressed as follows:

$$(\textbf{Impact index})_j = \left\| MSECR^{d}_{(ssi-cov)j} \right\|_2 = \sqrt{\sum_{d=1}^{S} \left(MSECR^{d}_{(ssi-cov)j} \right)^2} \tag{42}$$

By using the impact index that quantifies the MSECR of structural elements using the Euclidean norm under potential damage scenarios, it is possible to identify the most critical elements. In a real structure, the element with the highest impact index is considered a critical component and is identified as a suitable location for sensor installation to support SHM. The main focus of this study is to evaluate the effectiveness of structural monitoring with an emphasis on identifying critical members and assessing the reliability of damage detection and identification. To minimize the number of sensors required during response recording and monitoring, the proposed method recommends installing sensors at nodes common to critical elements or at least at one of the nodes connected to them. Accordingly, the proposed sensor placement process is divided into three consecutive steps, in which in the first step, the MSECR are calculated for all elements under each assumed damage scenario using Eq. (41). In the second step, the impact index for each element is calculated using Eq. (42), and in the third step, sensors are installed at the nodes associated with the most important elements to enable effective monitoring of the structure. In the case studies in section 4 , the effect of this index is clearly examined.

2.1.4. System Identification under Incomplete Data

After identifying the critical members and installing the sensors at the recommended DOFs, the recorded data does not fully cover the response of the structure, because the number of installed sensors is not enough to match the total DOFs of the structure. Therefore, to reconstruct the response of the entire structure, the Ref-SSI method can be used, focusing on a subset of sensor data, which are classified as reference and non-reference data. Using this method, the system is identified under different failure scenarios and with a limited number of sensors installed at recommended positions in the structure that ensure that the sensors are installed at the most sensitive degrees of freedom, and finally the MSECR is calculated for the structural members. Therefore, the outputs are expressed as follows, assuming the data obtained from the sensors as reference outputs (Peters and Rook, 2000):

$$y_k \equiv \begin{bmatrix} y_k^{ref} \\ y_k^{\sim ref} \end{bmatrix}, \qquad y_k^{ref} = L y_k, \qquad L \equiv [I_r 0] \tag{43}$$

Where $y_k^{ref} \in \mathbb{R}^{r \times 1}$ represents the reference outputs and $y_k^{-ref} \in \mathbb{R}^{(l-r) \times 1}$ represents the other outputs and $L \in \mathbb{R}^{r \times 1}$ is the reference output selection matrix. Reference data consist of a subset of data selected from the complete data of measurement channels. They act as a basis for projecting the data and reduce the dimensionality of the problem by constructing the Hankel matrix. Non-reference data are the remaining data that are not selected as reference data and their role in the identification process is indirect. However, if non-reference sensor data is missing or incomplete, one approach to fill in the gaps is to use data from a FE numerical model under dynamic analysis. This hybrid approach combines experimental and numerical data to enhance the Ref-SSI method's effectiveness. In this case, it is possible to provide the covariance matrix between the reference outputs and all the outputs, as well as the covariance matrix of the reference outputs with state variables in a next time step:

$$\Lambda_i^{ref} = E[y_{k+i} y_k^{ref^T}] = \Lambda_i L^T = CA^{i-1} G^{ref} \in \mathbb{R}^{l \times r} \tag{44}$$

$$\mathrm{G}^{ref} = E[x_{k+1} y_k^{ref^T}] = GL^T \in \mathbb{R}^{n \times r} \tag{45}$$

The outputs are collected in the Hankel matrix and can be presented as follows:

$$H \equiv \frac{1}{\sqrt{j}} \left[\begin{array}{cccc} y_0^{ref} & y_1^{ref} & \cdots & y_{j-1}^{ref} \\ y_1^{ref} & y_2^{ref} & \cdots & y_j^{ref} \\ \cdots & \cdots & \cdots & \cdots \\ y_{i-1}^{ref} & y_i^{ref} & \cdots & y_{i+j-2}^{ref} \\ \hline y_i & y_{i+1} & \cdots & y_{i+j-1} \\ y_{i+1} & y_{i+2} & \cdots & y_{i+j} \\ \cdots & \cdots & \cdots & \cdots \\ y_{2i-1} & y_{2i} & \cdots & y_{2i+j-2} \end{array} \right] \equiv \left(\frac{Y_{0|i-1}^{ref}}{Y_{i|2i-1}} \right) \equiv \left(\frac{Y_{\mathrm{p}}^{ref}}{Y_f} \right) \frac{\text{"}past\text{"}}{\text{"}future\text{"}} \tag{46}$$

In the following, the generalized observability matrix and the reference reversed extended stochastic controllability matrix based on the reference data can also be expressed as follows:

$$O_i = \begin{pmatrix} C \\ CA \\ CA^2 \\ \cdots \\ CA^{i-1} \end{pmatrix} \in \mathbb{R}^{li \times n} \tag{47}$$

$$C_i^{ref} \equiv \left(A^{i-1} G^{ref} \;\; A^{i-2} G^{ref} \;\; \cdots \;\; AG^{ref} \;\; G^{ref} \right) \in \mathbb{R}^{n \times ri} \tag{48}$$

The covariance values obtained from the output data by using of $\Lambda_i^{ref} = E[y_{k+i} y_k^{ref^T}]$ are collected in Toeplitz matrix:

$$T_{l|i} = \begin{pmatrix} \Lambda_i^{ref} & \Lambda_{i-1}^{ref} & \cdots & \Lambda_1^{ref} \\ \Lambda_{i+1}^{ref} & \Lambda_i^{ref} & \cdots & \Lambda_2^{ref} \\ \cdots & \cdots & \cdots & \cdots \\ \Lambda_{2i+1}^{ref} & \Lambda_{2i-2}^{ref} & \cdots & \Lambda_i^{ref} \end{pmatrix} \tag{49}$$

Using Eq. (46) and assuming that the data is ergodic and by applying the SVD method to the Toeplitz matrix, the separated and decomposed form of this matrix can be presented as follows:

$$T_{1|i}^{ref} = Y_f Y_p^{ref^T} = \begin{pmatrix} C \\ CA \\ CA^2 \\ \cdots \\ CA^{i-1} \end{pmatrix} \left(A^{i-1} G^{ref} \;\; A^{i-2} G^{ref} \;\; \cdots \;\; AG^{ref} \;\; G^{ref} \right) \tag{50}$$

$$T_{1|i}^{ref} = O_i C_i^{ref} \tag{51}$$

$$T_{1|i}^{ref} = USV^T = \begin{pmatrix} U_1 & U_2 \end{pmatrix} \begin{pmatrix} S_1 & 0 \\ 0 & 0 \end{pmatrix} \begin{pmatrix} V_1^T \\ V_2^T \end{pmatrix} = U_1 S_2 V_1^T \tag{52}$$

By equating Eqs. (51) and (52) can write:

$$O_i = U_1 S_1^{\frac{1}{2}}, \qquad C_i^{ref} = S_1^{1/2} V_1^T \tag{53}$$

Therefore, the state matrix A can be obtained by decomposing the new Toeplitz matrix with a shifted block as follows:

$$T_{2|i+1}^{ref} = O_i A C_i^{ref} \tag{54}$$

By solving Eq. (54) and considering Eq. (53), the state matrix can be rewritten in the following form:

$$A = O_i^{\dagger} T_{2|i+1}^{ref} C_i^{ref\dagger} = S_i^{-\frac{1}{2}} U_1^T T_{2|i+1}^{ref} V_1 S_i^{-\frac{1}{2}} \tag{55}$$

The mode shapes obtained from the reference data are defined as $\Phi_{ref-ssi}$.

2.1.5. Validation of Proposed Near-OSP Pattern

Given the importance of the issue, it is necessary to evaluate the reliability of the proposed process. For this purpose, the proposed location for sensor installation is matched with the optimal locations provided by the optimization process. Among these optimal sensor placement tools, the Genetic Algorithm (GA) is a widely used optimization method that, based on the principles of natural evolution, extracts optimal solutions by searching the space of possible solutions. This method starts by defining a set of data as an initial population and evaluates each generated solution using an objective function. Subsequently, by applying evolutionary operators such as selection, crossover, and mutation to the initial solutions, a new population of solutions is generated. This population evolves iteratively through repeated evaluation of the objective function and ensures convergence towards an optimal solution. The mathematical model of this problem is formulated as follows:

$$\max f(n_1,\ n_2, \ldots, n_s), \qquad s.t. \quad n_1,\ n_2, \ldots, n_s \in N \tag{56}$$

Where f is the objective function, that is determined according to the selected evaluation criterion for the optimization problem. According to the influencing factors in the proposed process, Modal Assurance Criterion (MAC) has been chosen as the evaluation criterion. This criterion is used to evaluate the correlation between the state shapes of the numerical model Φ_t and the state shapes of the experimental test $\Phi_{ref-ssi}$ which is obtained from the Ref-SSI method. MAC matrix components are defined as follows (Pastor et al., 2012):

$$MAC_{ij} = \frac{(\phi_t^T \phi_{(ref-ssi)})^2}{(\phi_t^T \phi_t)(\phi_{(ref-ssi)}^T \phi_{(ref-ssi)})} \tag{57}$$

Fitness Function: The off-diagonal elements in the MAC matrix express the correlation between two mode shape vectors. When $MAC_{ij} = 0$, two vectors are orthogonal. If N is the number of sensors available for installation in the structure, then the fitness function can be presented as follows:

$$f = 1 - RMS, \qquad RMS = \sqrt{\frac{1}{N(N-1)}\sum_{i=1}^{N}\sum_{j=1}^{N}\left(MAC_{ij}\right)^2}, i \neq j \tag{58}$$

Where RMS is the root mean square of the off-diagonal elements in the MAC matrix.

2.2. STEP 2: Damage identification process based on probabilistic approach:

Eqs. (34) and (35) are utilized to calculate the modal strain energy of the members in the healthy and damaged structures, with the difference that the mode shapes obtained from the Ref-SSI method are used to calculate the modal strain energy of the damaged state.

$$MSE^{d}_{(ref-ssi)j} = \sum_{i=1}^{m} \Phi^{d^T}_{(ref-ssi)i} K_j \Phi^{d}_{(ref-ssi)i} \tag{59}$$

Based on this, the amount of changes in the strain energy of the members can be presented in the form of the following relationship:

$$MSECR^{d}_{(ref-ssi)j} = max\left(0, \frac{\sum_{i=1}^{nm} NMSE^{d}_{(ref-ssi)ij} - \sum_{i=1}^{nm} NMSE^{u}_{ij}}{\sum_{i=1}^{nm} NMSE^{u}_{ij}}\right) \tag{60}$$

The application of a probabilistic framework and Bayesian strategy enhances the reliability of damage detection in the structure under investigation by effectively managing uncertainties through the integration of multiple data sources from various states. This probabilistic approach facilitates the differentiation between actual damage and false alarms arising from noise or the presence of a large number of degrees of freedom. In this approach, each mode of vibration is treated as an independent source of information. For each mode, the MSECR is calculated for all structural elements. These MSECR values are used as inputs to the Bayesian strategy to compute the probability of damage for each element. The framework of Bayesian theory can be presented as follows (Marwala, 2010; Guo and Li, 2012):

$$P(\theta|D) = \frac{P(D|\theta)P(\theta)}{P(D)} \tag{61}$$

Here, $P(\theta)$ is the probability distribution function of the design space in the absence of every data, which is also called the prior distribution function and $D = (y_1, \ldots, y_N)$ is a matrix containing data. The term $P(\theta|D)$ is the posterior probability distribution function after observing the data and $P(D|\theta)$ is the probability distribution function and $P(D)$ is the normalized factor. Information fusion methods can combine data extracted from multiple information sources to obtain more accurate results and a general decision is made based on the combination of all or part of the data. It is assumed that L is an independent source of information $S_1, S_2, \ldots, S_L$ and N is the number of propositions or elements $A_1, A_2, \ldots, A_N$. In Bayesian theory, the prior probability of each proposition is denoted by $P(A_i)(i = 1,2, \ldots, N)$ and given that at the same period of time the values of the conditional probability $P(S_1, S_2, \ldots, S_L|A_i)$ are already known, therefore, the Bayesian combination can be presented as follows for the probability of a proposition under multiple information sources:

$$P(A_i|S_1, S_2, .., S_L) = \frac{\prod_{k=1}^{L} P(S_k|A_i)P(A_i)}{\sum_{j=1}^{N} \prod_{k=1}^{L} P(S_k|A_j)P(A_j)} \tag{62}$$

By defining the modal strain energy index for each data source under the framework of each mode, the data set can be expressed as follows:

$$S_L = \{MSECR_{L1}, MSECR_{L2}, \ldots, MSECR_{Lj}\} \tag{63}$$

The probability of damage for each structural element in each mode can be presented as follows:

$$P_L(A_i) = \frac{MSECR_{Lj}}{\sum_{j=1}^{n} MSECR_{Lj}}, j = 1, \ldots, n \tag{64}$$

Where $P_L(A_i)$ is the calculated damage probability of member A_i from information source S_L which is defined in Eq. (41) and finally by combining the damage probability of members from different information sources, the damage probability of each member can be presented. The term $P(A_i)$ is equivalent to the prior damage probability of the element and is defined as follows:

$$P(A_i) = \frac{1}{n}, i = 1,2, \ldots, N \tag{65}$$

Here, *N* defines the number of elements of the structure and ultimately the elements that based on the assumption of the response of the structure in the form of the first three modes have the highest probability of damage are identified as damaged. In Figure 1 the flowchart of the proposed algorithm for determining important members and the process of identifying damage in the structure is presented.

3. Numerical Model and Results

In this section, the level of reliability and results of the structural damage identification procedure will be investigated using the proposed technique for optimal placement of the sensor. The dynamic analysis conducted using MATLAB software with the specifications of the SSI approach, and the FEM has been used for all structure simulations. All time-domain responses used for SHM were generated by applying uncorrelated Gaussian white-noise excitation to all DOFs of the finite-element model and computing the resulting acceleration response by modal superposition. The modal coordinates were obtained by discrete convolution of the modal impulse response with white-noise forcing, and acceleration time histories at each DOF were generated via modal superposition. The simulated acceleration series are sampled for specific time intervals are used as inputs to the SSI-COV and REF-SSI identification procedures. This approach models ambient operational excitation and follows standard output-only modal identification practice.

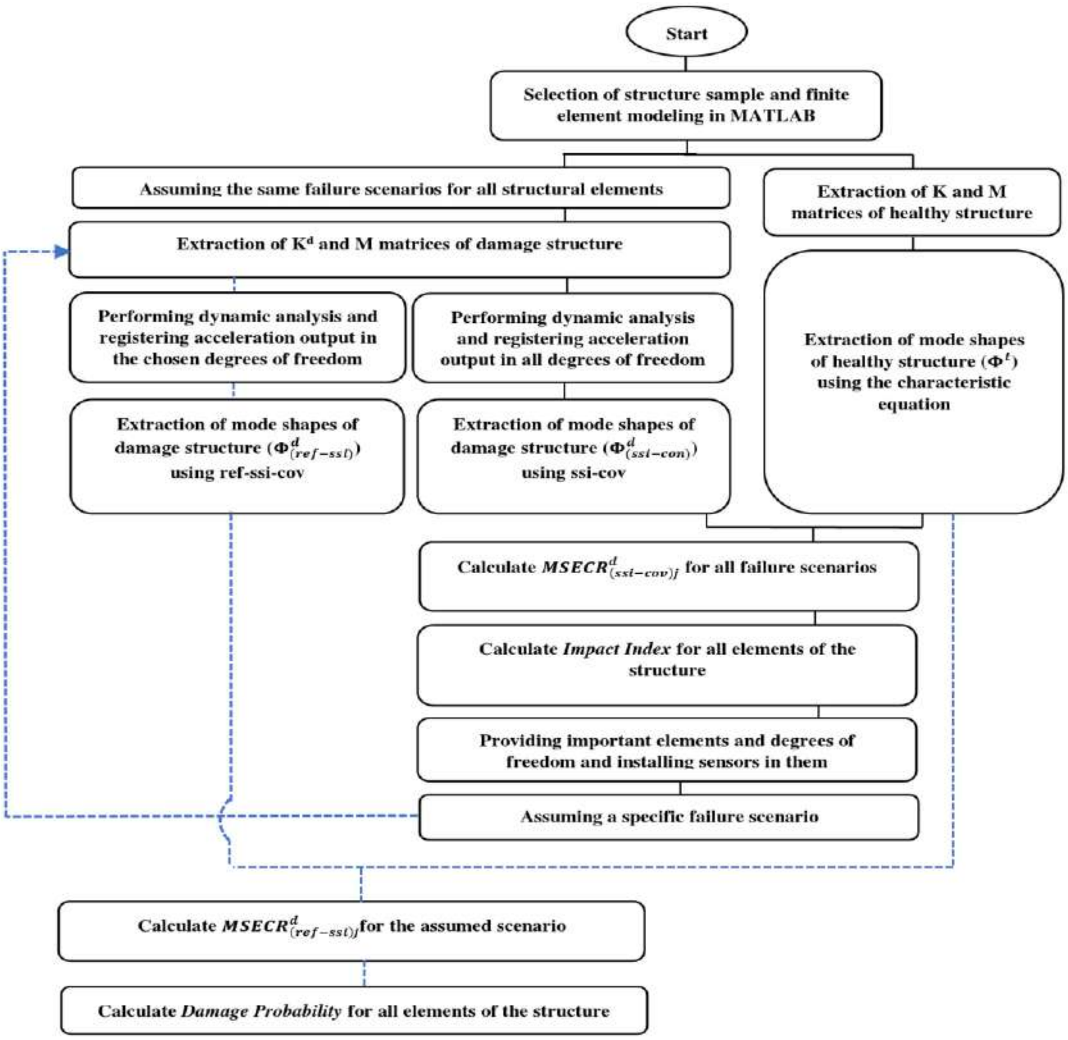

Fig. 1. Flowchart of the proposed algorithm to determine important members for robust near-optimal sensor placement and the process of identifying damage in the structure

For each case study, (i) the modal identification results obtained by SSI-COV method are validated, (ii) the Near-optimal sensor configuration is obtained through the proposed framework with stochastic damage sampling, and (iii) the damage localization performance is evaluated using REF-SSI combined with the Bayesian integration strategy MSECR. To account for environmental conditions, the effect of noise on the results of the proposed process is investigated. Therefore, in the damage detection section, which is based on the sensor layout pattern introduced, the REF-SSI analyses are re-run with zero-mean and Gaussian sensor noise applied to each acceleration channel signal-to-noise ratio (SNR = 40 and 30 dB). For each SNR level, N = 50 Monte-Carlo runs are performed to obtain robust statistics (mean ± standard deviation) of REF-SSI detection, MSECR/impact index, and Bayesian damage probabilistic. The SNR is defined as:

$$SNR_{db} = 10\log_{10}\left(\frac{\mathbb{E}[a^2(t)]}{\mathbb{E}[n^2(t)]}\right) \tag{66}$$

Where $a(t)$ is the clean (noise-free) acceleration and $n(t)$ is the additive measurement noise. For each prescribed SNR the noisy signals were generated as $\tilde{a}(t) = a(t) + n(t)$.

3.1.Case Study on 2D-Truss

In this example, a two-dimensional truss with 14 nodes and 31 elements is considered (Kaveh and Ghazaan, 2015). Each node has two horizontal and vertical degrees of freedom, therefore the structure has 25 active degrees of freedom, which degrees of freedom 1, 2 and 28 are assumed to be constrained due to the support conditions. The cross-sectional area, modulus of elasticity and density of the members are 0.004 m^2, 70 *Gpa* and 2770 kg/m^3, respectively. A schematic representation of the described truss is provided in Figure 2.

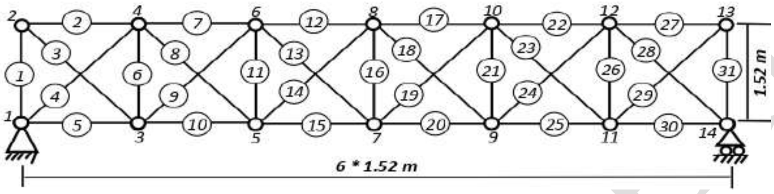

Fig.2. 31-elements 2D-truss

The first 10 natural frequencies of the structure are summarized in Table 1. Additionally, the stabilization diagram depicting the system identification parameters, specifically the natural frequencies obtained using the SSI-COV method, is illustrated in Figure 3(a). The results demonstrate good agreement with the theoretical predictions. To validate the identified system parameters, the MAC can be employed, which demonstrates a strong correlation between the theoretical and experimental mode shape vectors, as illustrated in Figure 3(b). This agreement confirms the accuracy of the structural modeling and the correct implementation of the stochastic subspace identification method through the developed MATLAB code.

Table.1. The first 10 natural frequencies of the 31-element 2D-truss

Mode	1	2	3	4	5	6	7	8	9	10
Frequency(Hz)	36.42	76.09	133.81	223.37	250.18	359.35	372.86	443.54	478.41	508.00

Subsequently, the impact index values for each element are computed, considering potential failure scenarios based on the proposed methodology, and the results are presented in Figure 4.

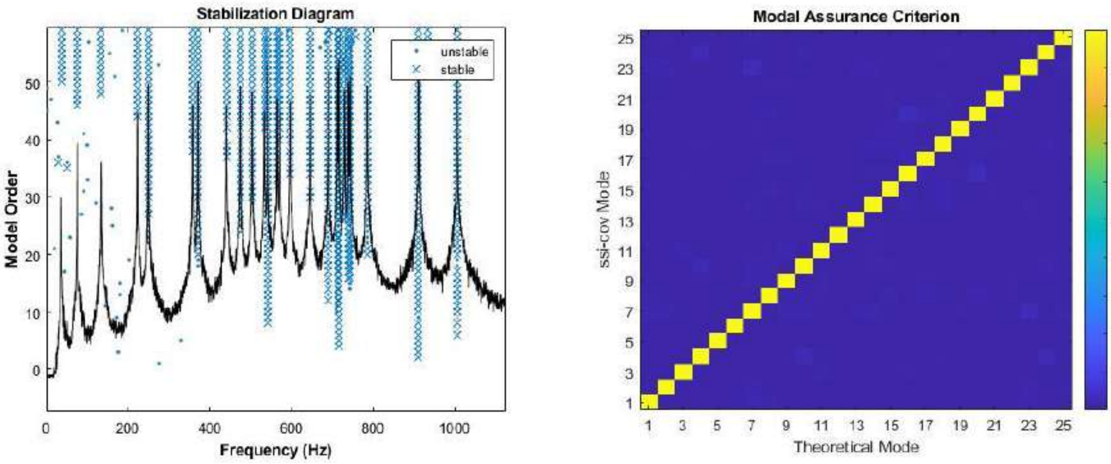

(a) (b)

Fig. 3. (a): Stabilization Diagram of SSI-COV method, (b): MAC-comparison between estimated mode shapes vectors using the identification approach (SSI-COV) with theoretical mode of 31-element 2D-truss

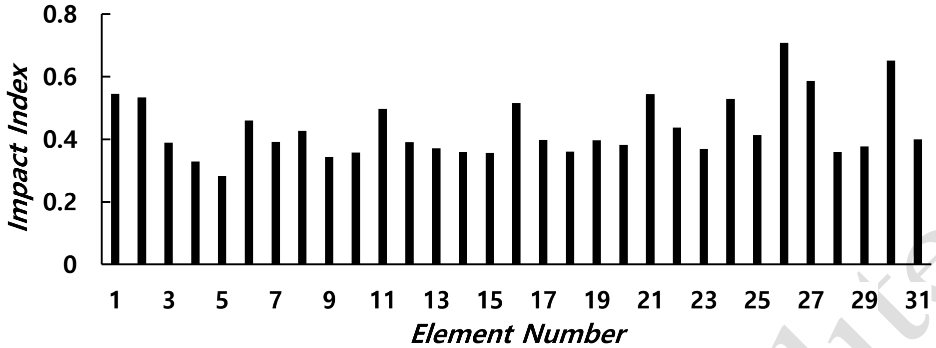

Fig. 4. impact index (Proposed criterion) based on modal strain energy change ratio (MSECR) index for 31-element 2D-truss

The selection of nodes for sensor installation is based on two key principles: first, at least one node connected to the element with the highest impact index should be selected; second, the total number of nodes should be minimized, while also considering the support conditions of the structure. Regarding the specific selection of nodes and the associated degrees of freedom for elements with the highest impact index, it can be stated that, based on the first principle, node 4 is selected. This node connects elements 2, 6, and 8 and provides both horizontal and vertical degrees of freedom, making it suitable for recording the system response and installing the sensor. Due to the nature of truss elements, the horizontal strain in element 2, the vertical strain in element 6, and both horizontal and vertical strains in element 8 can be recorded through the degrees of freedom available at node 4. For element 11, placing a sensor on the vertical degree of freedom at node 6 is sufficient to capture the vertical strain in that element. Table 2 presents a comparison between the results of the proposed sensor placement method and the results of the optimization process using the genetic algorithm, with the explanation that in the proposed method there is no cyclic or iterative process to reach the solution, but at the same time the results are close to optimal.

Table 2. Comparison of suggested degrees of freedom for sensor installation using proposed flowchart and genetic algorithm in 31-elements 2D-truss

Method		Degrees of freedom (node number/direction)
sensor configurations proposed method		2y,4x,4y,6y,8y,9y,11x,12x,12y
sensor configurations of Genetic Algorithm	Fitness function value	2x,4y,6y,8y,10x,11x,12x,12y,13x
	0.91	

Table 3. Assumed damage scenarios in 31-elements 2D-truss

Scenario of Damage	Element number	Damage precent
1	21	20

2	11	20
	25	15
3	2	20
	6	15
	27	10

Further, in order to validate the processes of optimal sensors placement and correct identification of damaged elements in the structure, different damage scenarios are considered in Table 3. After considering various damage scenarios for elements, the index of modal strain energy Changes and the damage probability of elements are presented in Figures 5(a)-(f).

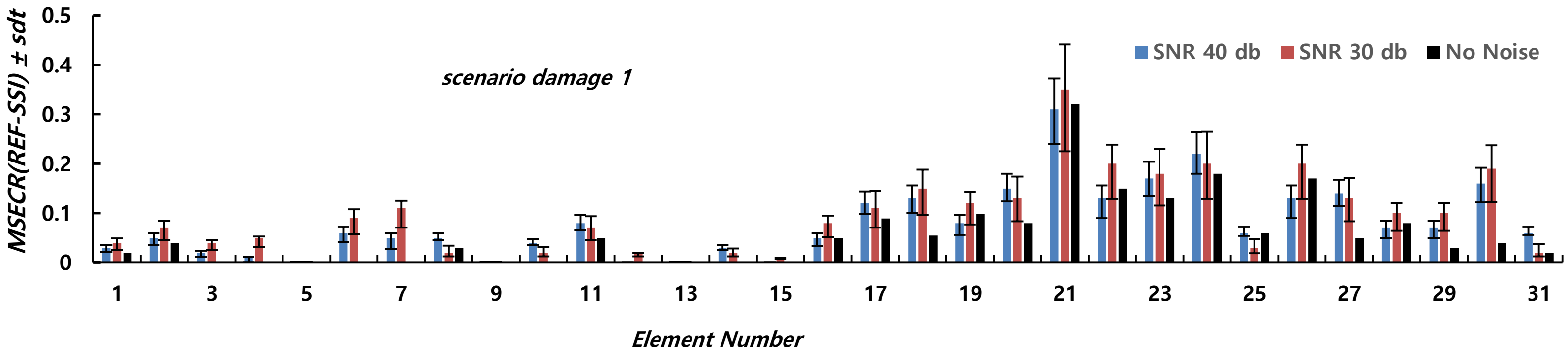

SNR 40 db
SNR 30 db
No Noise
scenario damage 1
MSECR(REF-SSI) ± sdt
Element Number

(a)

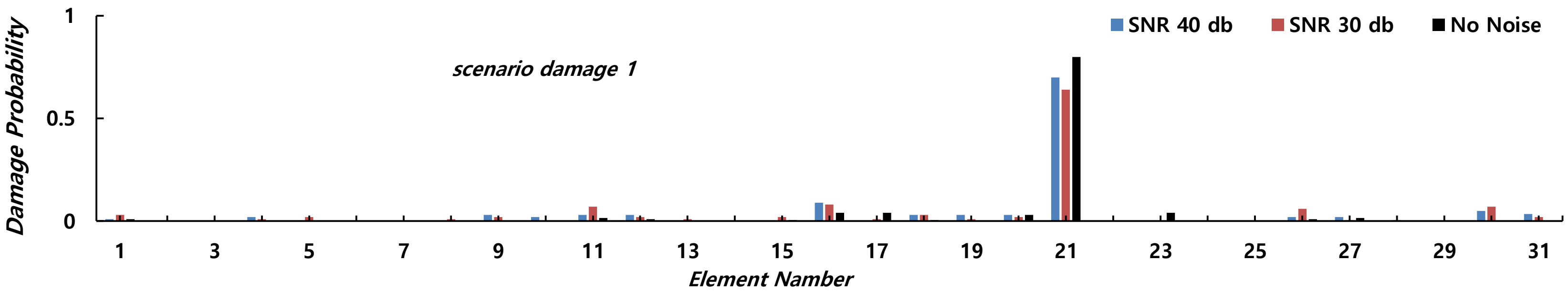

SNR 40 db
SNR 30 db
No Noise
scenario damage 1
Damage Probability
Element Namber

(b)

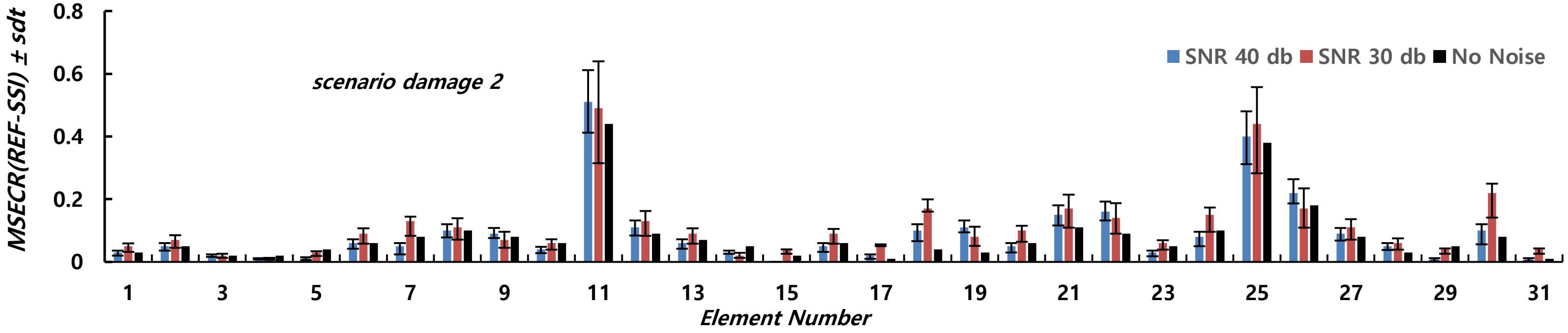
MSECR(REF-SSI) ± sdt
scenario damage 2
SNR 40 db
SNR 30 db
No Noise
Element Number
(c)

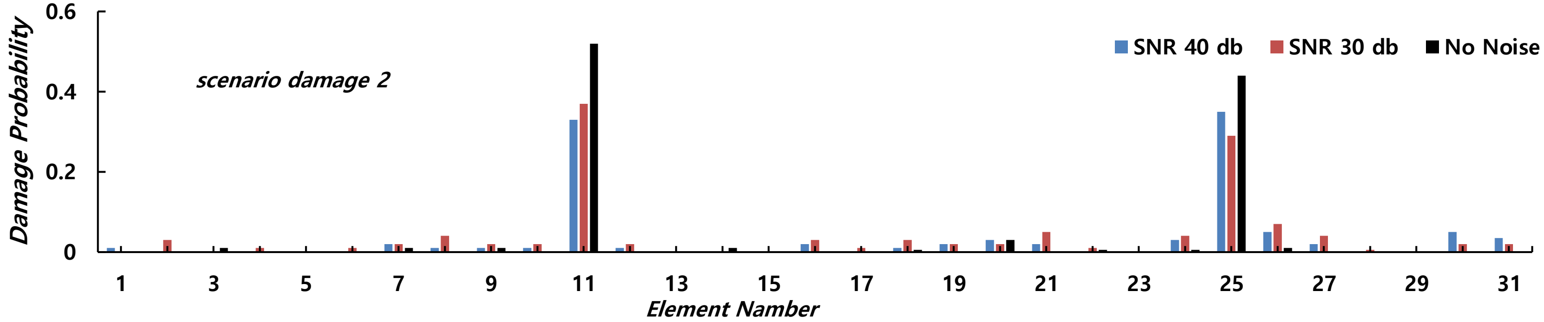
Damage Probability
scenario damage 2
SNR 40 db
SNR 30 db
No Noise
Element Namber
(d)

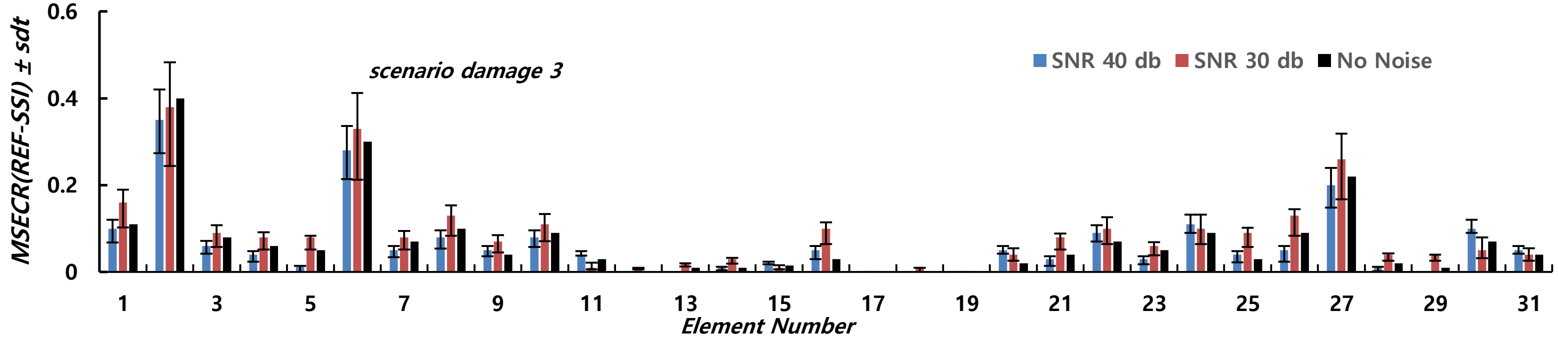

(e)

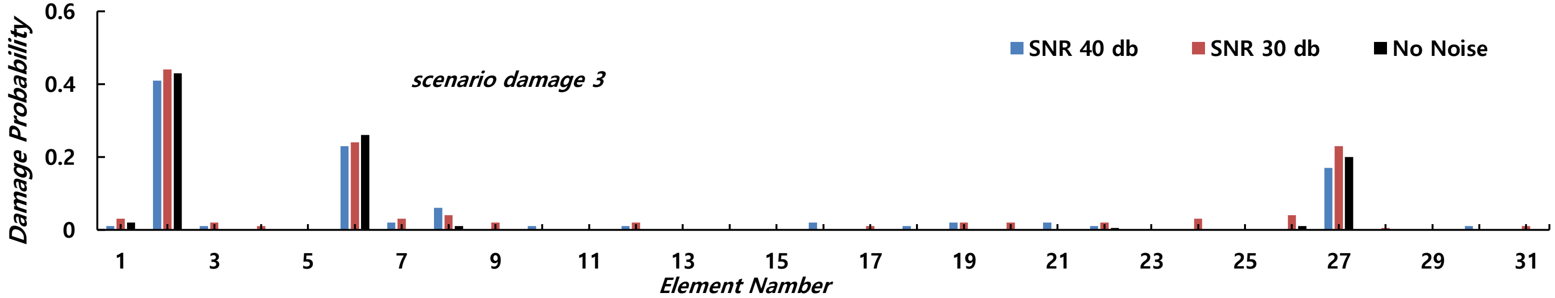

(f)

Fig. 5; (a), (c), and (e) ***MSECR**$_{ref\text{-}ssi}$* **± sdt** ; (b), (d) , and (f) ***Damage Probability*** respectively in scenarios 1, 2, and 3 in 31-element 2D-truss

The graph of variations in the MSECR of structural members under different damage scenarios indicates that, in addition to the damaged elements, adjacent undamaged members may also be incorrectly identified as damaged due to the influence of nearby damage. To mitigate such false positives and enhance the accuracy of damage identification, a probabilistic approach is adopted by integrating the Bayesian strategy with the MSECR results. This method enables a more realistic assessment by accounting for uncertainties associated with various damage scenarios. It consistently assigns higher probabilities of damage to genuinely damaged members compared to intact ones, thereby validating the reliability of the identification process. Moreover, the results confirm that the proposed sensor configuration demonstrates robustness across diverse damage conditions and ensures the collection of reliable data to support accurate structural damage detection.

3.2.Case Study on Tower

In this case, a 2D truss tower with 22 nodes, with two horizontal and vertical degrees of freedom for each node and 47 elements, is considered (Nouri et al., 2014). The structure has 44 degrees of freedom, and the modulus of elasticity and density of the members are 30000 *ksi* and 0.3 Ib/in^3, respectively. The assumed constraints in this example are applied in the form of displacement constraints on nodes, which are degrees of freedom 1, 2, 43, and 44 (horizontal and vertical degrees of freedom of nodes 1 and 22). Therefore, the truss structure has 40 active degrees of freedom, and the described truss is presented in Figure 6.

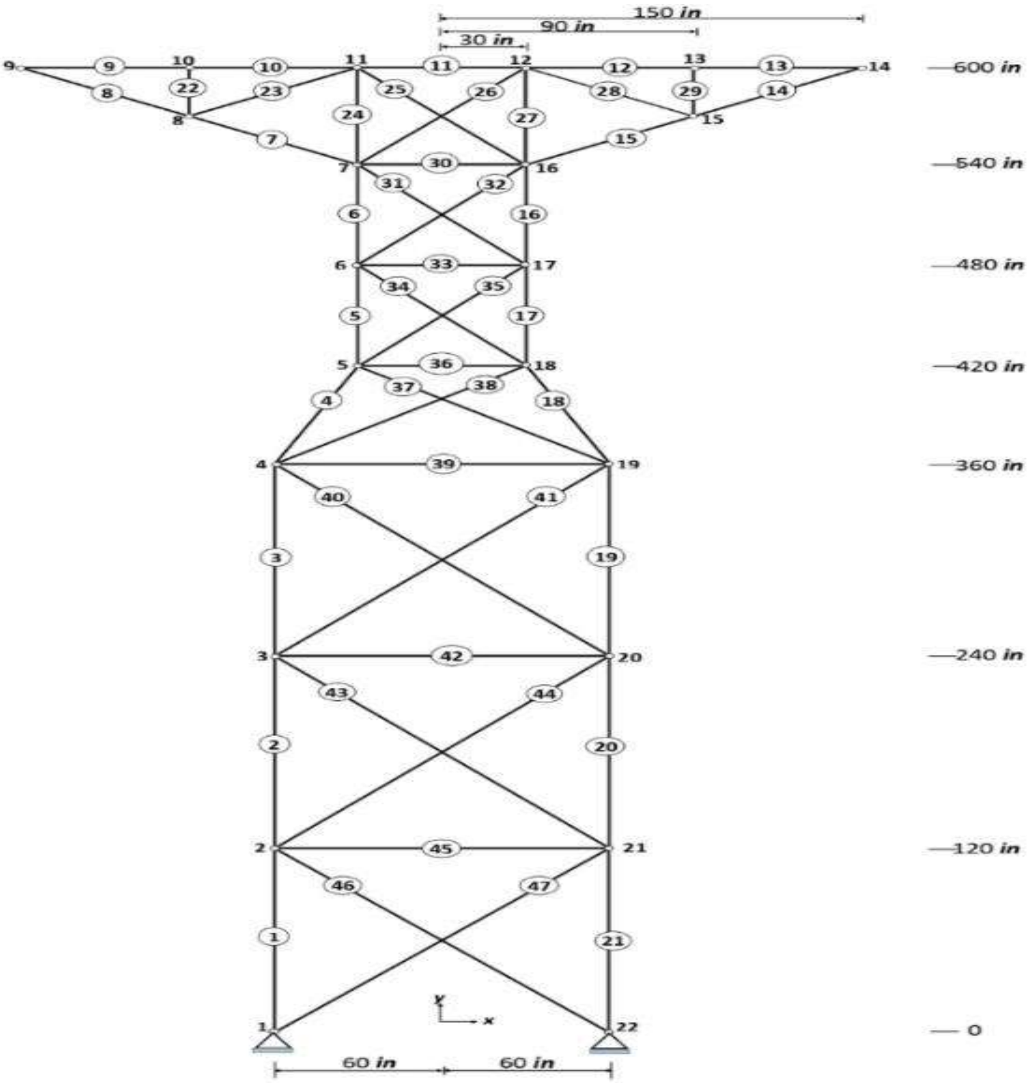

Fig. 6, Tower (47-element 2D-truss)

The first 10 natural frequencies of the structure are summarized in Table 4. Additionally, the stabilization diagram depicting the system identification parameters, specifically the natural frequencies obtained using the SSI-COV method, is illustrated in Figure 7(a). The results exhibit strong agreement with the theoretical predictions.

Table 4. The first 10 natural frequencies of the Tower (47-element 2D-truss)

Mode	1	2	3	4	5	6	7	8	9	10
Frequency(Hz)	0.36	1.41	2.10	3.31	5.37	5.47	7.40	9.14	10.72	1169

The MAC presented in Figure 7(b) shows a good agreement between the numerical and SSI-COV results for the described truss. In the following, using equation 42, the value of the impact Index of all the members of the structure is calculated and presented in Figure 8. As can be seen, elements number 7, 8, 9, 10, 11, 12, 13, 14, 15, 22, 23, 24, 27, 28, 29, 30 and 33 have a higher impact index than the other members. According to the principles assumed for the proposed process of sensor installation in nodes related to structural elements, a total of 11 sensors have been installed in related degrees of freedom.

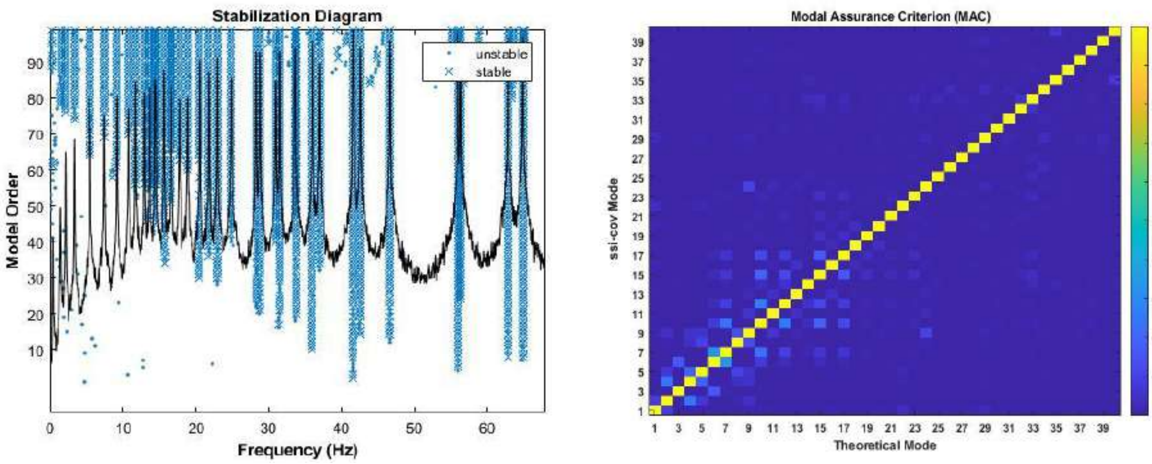

(a) (b)

Fig. 7.(a): Stabilization Diagram of SSI-COV in tower, (b): MAC–comparison between estimated mode shapes vectors using the identification approach (SSI-COV) and theoretical state of tower

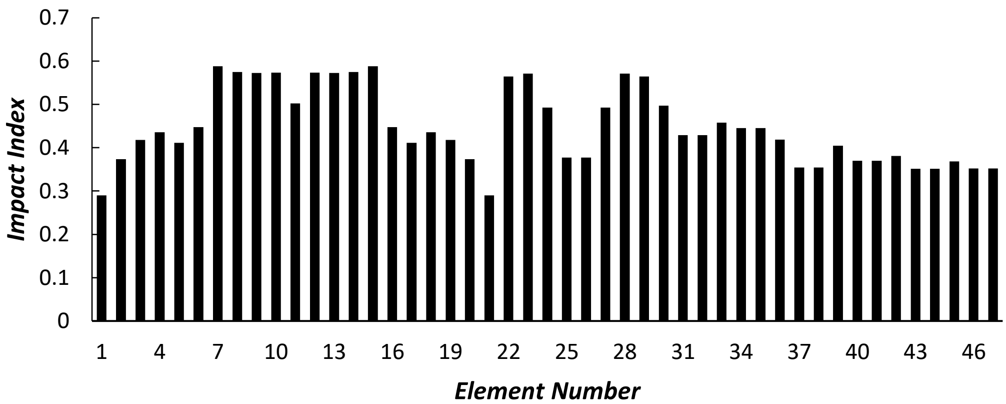

Fig. 8, impact index (Proposed criterion) based on modal strain energy change ratio (MSEC) index for a tower

In Table 5, the results of the proposed method for providing the optimal sensor installation location are compared with the results of the genetic algorithm. In order to evaluate the efficiency of the proposed flowchart for identifying structural damage using sensors installed in the degrees of freedom provided by the proposed impact index, various scenarios of structural failure have been considered in the form of Table 6. The figures related to MSECR index and damage probability of structural members under the assumed damage scenarios are presented in Figures 9(a)-(f).

Table 5. Comparison of suggested degrees of freedom for sensor installation using proposed flowchart and

genetic algorithm in Tower (47-element 2D-truss)

Method		**Degrees of freedom (node number/direction)**
sensor configurations proposed method		7x, 7y, 8y, 9x, 11x, 12x, 14x, 15y, 16x, 16y, 17x
sensor configurations of Genetic Algorithm optimization	Fitness function value	5y, 7x, 8x, 9x, 10y, 11y, 12x, 14x, 15y, 16y, 17x
	0.83	

Table 6. Assumed damage scenarios in Tower (47-element 2D-truss)

scenario of Damage	**element number**	**Damage precent**
1	25	20
2	18	15
	30	20
3	2	20
	13	15
	33	10

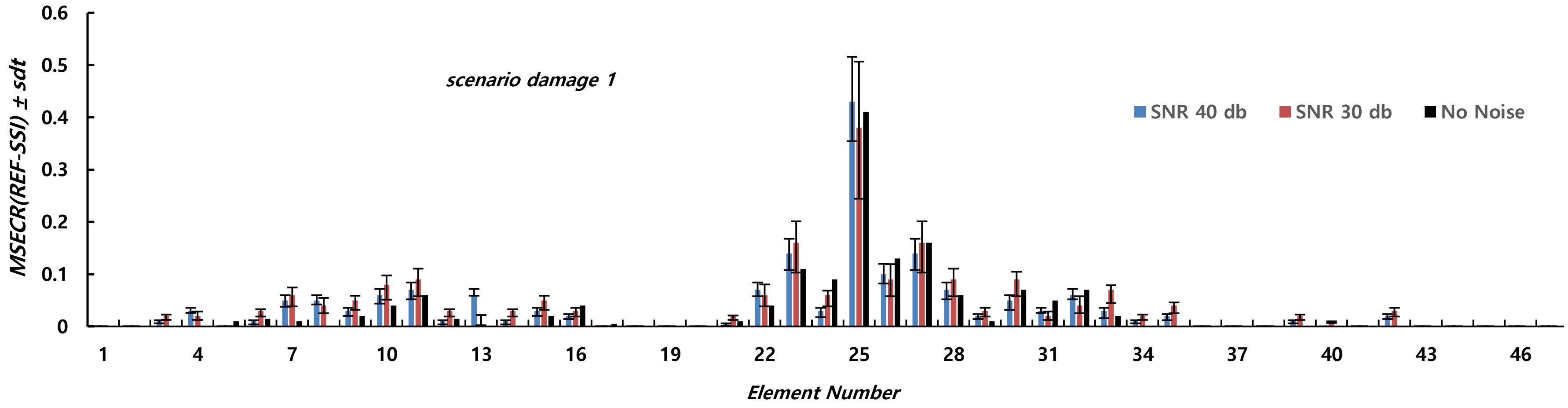

scenario damage 1
SNR 40 db
SNR 30 db
No Noise
MSECR(REF-SSI) ± sdt
Element Number

(a)

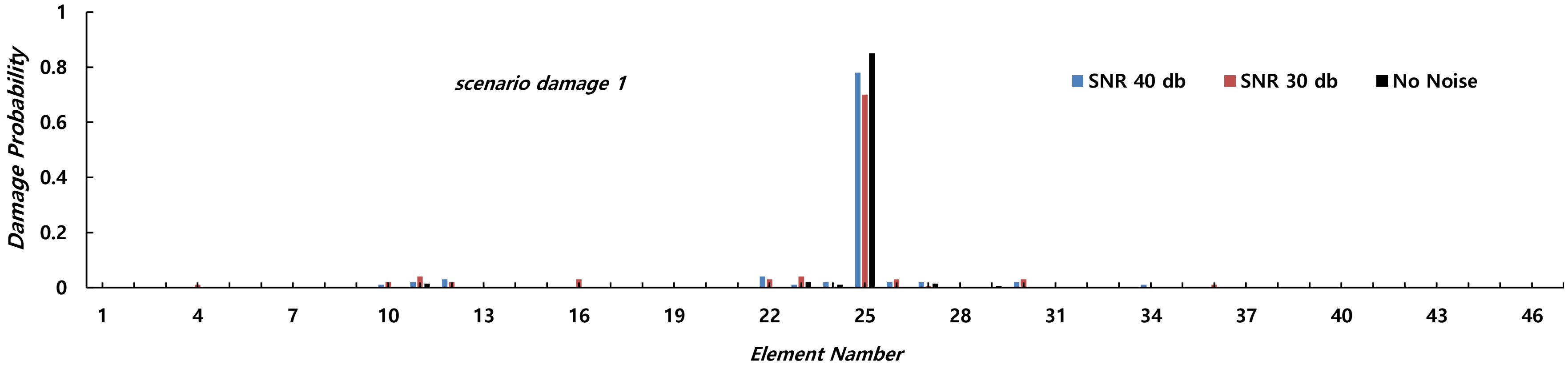

scenario damage 1
SNR 40 db
SNR 30 db
No Noise
Damage Probability
Element Namber

(b)

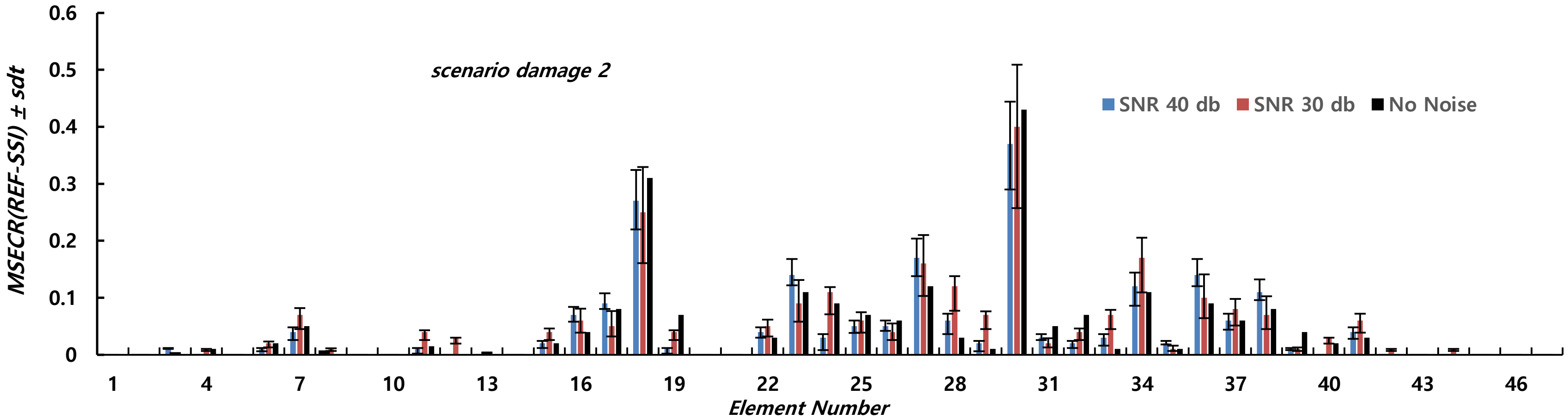
scenario damage 2
SNR 40 db
SNR 30 db
No Noise
MSECR(REF-SSI) ± sdt
Element Number
0
0.1
0.2
0.3
0.4
0.5
0.6
1
4
7
10
13
16
19
22
25
28
31
34
37
40
43
46

(c)

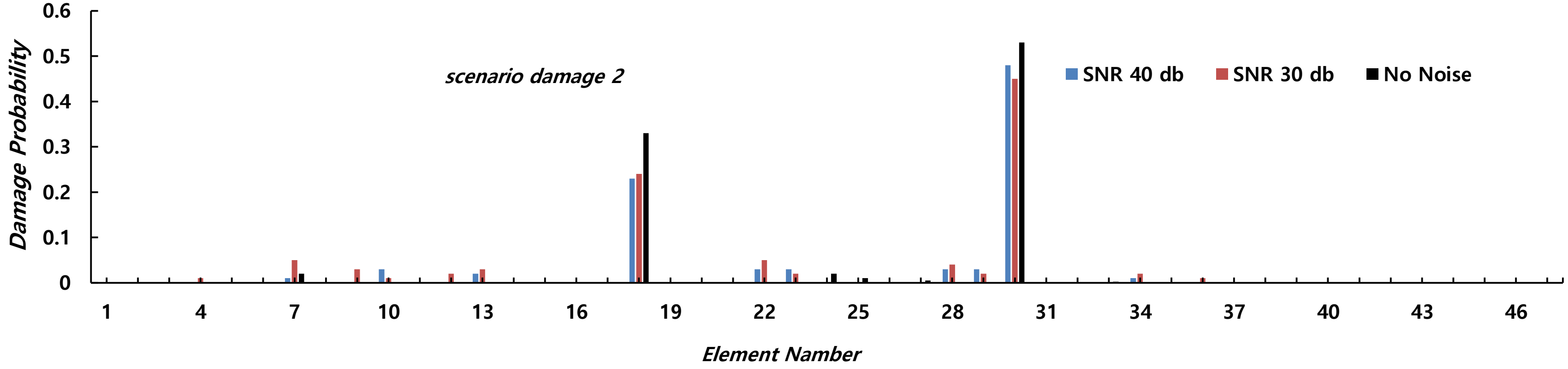

Damage Probability
scenario damage 2
SNR 40 db
SNR 30 db
No Noise
0.6
0.5
0.4
0.3
0.2
0.1
0
1
4
7
10
13
16
19
22
25
28
31
34
37
40
43
46
Element Namber

(d)

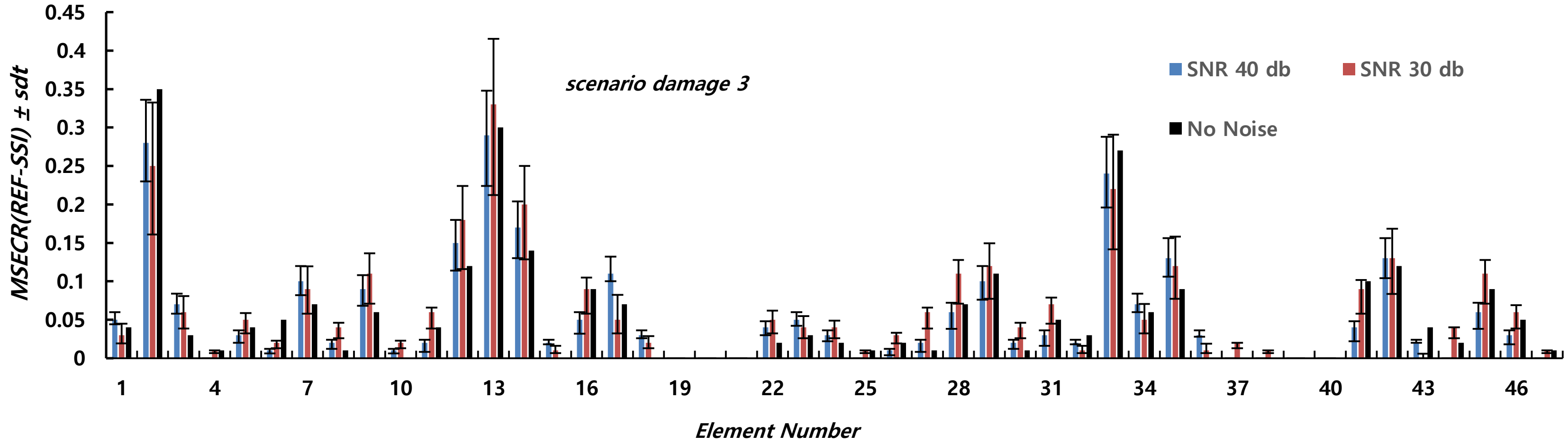

MSECR(REF-SSI) ± sdt
scenario damage 3
SNR 40 db
SNR 30 db
No Noise
0.45
0.4
0.35
0.3
0.25
0.2
0.15
0.1
0.05
0
1
4
7
10
13
16
19
22
25
28
31
34
37
40
43
46
Element Number

(e)

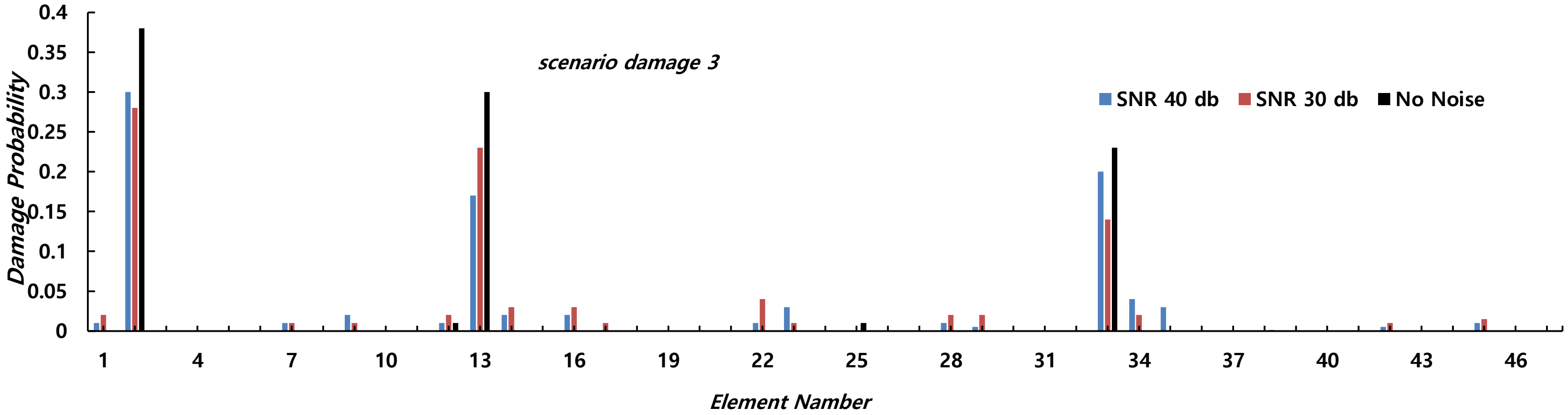

(f)

Fig. 9; (a), (c), and (e) ***MSECR$_{ref\text{-}ssi}$*** **± sdt** ; (b), (d) , and (f) ***Damage Probability*** respectively in scenarios 1, 2, and 3 in 47-element 2D-truss

According to the results obtained, and despite the complexity and increase in the number of structural members under study, in this case too, by using the Bayesian strategy and calculating the probability of damage of structural elements, the damaged members can be clearly identified. This not only increases the reliability of the proposed process for structural damage identification under uncertainties arising from different damage scenarios, but also confirms the operational efficiency of this process.

4. Conclusion

In this study, a robust and near-optimal sensor placement methodology was developed to enhance the reliability of structural health monitoring (SHM) under uncertainty arising from possible damage scenarios. By utilizing changes in modal strain energy (MSE) and introducing an impact index across all structural members, critical locations for sensor installation were identified. The proposed approach demonstrates resilience to modeling uncertainties and potential failure scenarios, ensuring effective system identification with a minimal number of strategically placed sensors. The effectiveness of the sensor layout was validated through comparison with a Genetic Algorithm (GA)-based optimization framework, confirming the near-optimal nature of the proposed configuration. The noise resistance is demonstrated through Monte-Carlo simulations (N = 50) and applying Gaussian sensor noise at SNR = 40 and 30 dB: The optimized layouts and Bayesian fusion provide almost reliable localization at the desired SNR levels, which shows an increase in the reliability of the proposed flowchart. Furthermore, the integration of a Bayesian strategy with the MSE change index allowed for probabilistic damage diagnosis, offering a clear distinction between healthy and damaged members even under complex conditions. While the present study focuses on ideal structural behavior and perfect sensor conditions, real-world implementations may require further investigation. Future research could extend the framework into areas such as adaptive sensing strategies or the integration of possible damage scenarios, which can be much more complex in number and combination in real-world conditions. Overall, the methodology presented here provides a practical and theoretically grounded tool for resilient and efficient SHM, contributing to more reliable damage detection in structural systems. the subject of limitations and particularly comprehensive and empirical evaluation as a planned follow - up with a combination of complex and weighted scenarios (including extreme weighting) for a more specific paper is appropriate and necessary.

6. REFERENCES

Arefi, S. L., Gholizad, A., & Seyedpoor, S. M. (2020), "A modified index for damage detection of structures using improved reduction system method". Smart Structures and Systems, 25(1), 1-25. https://doi.org/10.12989/sss.2020.25.1.001

An, H., Youn, B. D., & Kim, H. S. (2022), "A methodology for sensor number and placement optimization for vibration-based damage detection of composite structures under model uncertainty". Composite Structures, 279, 114863. https://doi.org/10.1016/j.compstruct.2021.114863

Avci, O., Abdeljaber, O., Kiranyaz, S., Hussein, M., Gabbouj, M., & Inman, D. J. (2021). A review of vibration-based damage detection in civil structures: From traditional methods to Machine Learning and Deep Learning applications. Mechanical systems and signal processing, 147, 107077. https://doi.org/10.1016/j.ymssp.2020.107077

Barman, S. K., Mishra, M., Maiti, D. K., & Maity, D. (2021). "Vibration-based damage detection of structures employing Bayesian data fusion coupled with TLBO optimization algorithm". Structural and Multidisciplinary Optimization, 64(4), 2243-2266. https://doi.org/10.1007/s00158-021-02980-6

Barthorpe, R. J., & Worden, K. (2020). "Emerging trends in optimal structural health monitoring system design: From sensor placement to system evaluation". Journal of Sensor and Actuator Networks, 9(3), 31. https://doi.org/10.3390/jsan9030031

Behtani, A., Tiachacht, S., Khatir, S., Slimani, M., Mansouri, L., Bouazzouni, A., & Abdel Wahab, M. (2020). "The sensitivity of modal strain energy for damage localization in composite stratified beam structures". In Proceedings of the 13th International Conference on Damage Assessment of Structures: DAMAS 2019, 9-10 July 2019, Porto, Portugal (pp. 863-874). Springer Singapore. https://doi.org/10.1007/978-981-13-8331-1_69

Brincker, R., & Ventura, C. (2015). "Introduction to operational modal analysis". John Wiley & Sons. https://doi.org/10.1002/9781118535141

Cascone, D., Navarra, G., Oliva, M., & Lo Iacono, F. (2020). "Influence of user-defined parameters using stochastic subspace identification (SSI)". In Proceedings of XXIV AIMETA Conference 2019 24 (pp. 1567-1582). Springer International Publishing. https://doi.org/10.1007/978-3-030-41057-5_127

Chen, C. T. (1984), "Linear system theory and design". Saunders college publishing. https://dl.acm.org/doi/abs/10.5555/542626

Das, S., & Saha, P. (2022). "Performance of Optimal Sensor Placement Strategies for Damage Detection in Civil Engineering". In Recent Developments in Sustainable Infrastructure (ICRDSI-2020)—Structure and Construction Management: Conference Proceedings from ICRDSI-2020 Volume 1 (pp. 269-279). Singapore: Springer Nature Singapore. https://doi.org/10.1007/978-981-16-8433-3_24

Ewins, D. J. (2009), "Modal testing: theory, practice and application". John Wiley & Sons.

Foti, D., Gattulli, V., & Potenza, F. (2014). "Output-only identification and model updating by dynamic testing in unfavorable conditions of a seismically damaged building". Computer-Aided Civil and Infrastructure Engineering, 29(9), 659-675. https://doi.org/10.1111/mice.12071

Frigui, F., Faye, J.P., Martin, C., Dalverny, O., Pérès, F. and Judenherc, S. (2018), "Global methodology for damage detection and localization in civil engineering structures", Eng. Struct., 171, 686-695. https://doi.org/10.1016/j.engstruct.2018.06.026

Ghafouri, H. Reza , Khajehdezfuly, A. and Saadat Poor, O. (2024). Damage Detection of Truss Bridges Using Wavelet Transform of Rotation Signal. Civil Engineering Infrastructures Journal, 57(1), 17-31. https://doi: 10.22059/ceij.2023.349207.1870

Gharehbaghi VR, Noroozinejad Farsangi E, Noori M, Yang TY, Li S, Nguyen A, Málaga-Chuquitaype C, Gardoni P, Mirjalili S (2022) A critical review on structural health monitoring: Definitions, methods, and perspectives. Arch Comput Methods Eng 29(4):2209–2235. https://doi.org/10.1007/s11831-021-09665-9

Ghosh, A., Chakraborty, A., & Dutta, A. (2022). "Experimental Verification of Improved SSI-COV Method for Health Monitoring of Base-Excited RC Structures". In Symposium in Earthquake Engineering (pp. 273-283). Singapore: Springer Nature Singapore. https://doi.org/10.1007/978-981-99-1608-5_20

Guo, H. Y., & Li, Z. L. (2012), "Structural damage identification based on Bayesian theory and improved immune genetic algorithm". Expert Systems with Applications, 39(7), 6426-6434.

https://doi.org/10.1016/j.eswa.2011.12.023
Hassani, S., & Dackermann, U. (2023). “A Systematic Review of Optimization Algorithms for Structural Health Monitoring and Optimal Sensor Placement”. Sensors, 23(6), 3293. https://doi.org/10.3390/s23063293
Hou, R., & Xia, Y. (2021). “Review on the new development of vibration-based damage identification for civil engineering structures”: 2010–2019. Journal of Sound and Vibration, 491, 115741. https://doi.org/10.1016/j.jsv.2020.115741
Juang, J. N. (1994), “Applied system identification”. Prentice-Hall, Inc.
Kahouadji, A., Tiachacht, S., Slimani, M., Behtani, A., Benaissa, B., Khatir, T., & Noori, M. (2023). “6 Structural health monitoring of steel plates using modified modal strain energy indicator and optimization algorithms”. Data-Centric Structural Health Monitoring: Mechanical, Aerospace and Complex Infrastructure Systems. Walter de Gruyter GmbH & Co KG. https://doi.org/10.1515/9783110791426-006
Katam R, Pasupuleti VDK, Kalapatapu P (2023) A review on structural health monitoring: past to present. Innov Infrastruct Solut 8(9):248. https://doi.org/10.1007/s41062-023-01217-3
Kaveh, A., & Ghazaan, M. I. (2015). A comparative study of CBO and ECBO for optimal design of skeletal structures. Computers & Structures, 153, 137-147. https://doi.org/10.1016/j.compstruc.2015.02.028
Khatir, S., Wahab, M. A., Boutchicha, D., & Khatir, T. (2019). “Structural health monitoring using modal strain energy damage indicator coupled with teaching-learning-based optimization algorithm and isogoemetric analysis”. Journal of Sound and Vibration, 448, 230-246. https://doi.org/10.1016/j.jsv.2019.02.017
Liesecke, L., Jonscher, C., Grießmann, T., & Rolfes, R. (2023). “Investigations of Mode Shapes of Closely Spaced Modes from a Lattice Tower Identified Using Stochastic Subspace Identification”. In International Conference on Experimental Vibration Analysis for Civil Engineering Structures (pp. 529-538). Cham: Springer Nature Switzerland. https://doi.org/10.1007/978-3-031-39109-5_54
Magalhães, F., Cunha, Á., & Caetano, E. (2012). “Vibration based structural health monitoring of an arch bridge: From automated OMA to damage detection”. Mechanical Systems and signal processing, 28, 212-228. https://doi.org/10.1016/j.ymssp.2011.06.011
Mao, J., Yang, C., Wang, H., Zhang, Y., & Lu, H. (2022). “Bayesian operational modal analysis with genetic optimization for structural health monitoring of the long-span bridge”. International Journal of Structural Stability and Dynamics, 22(05), 2250051. https://doi.org/10.1142/S0219455422500511
Marwala, T. (2010), “Finite element model updating using computational intelligence techniques: applications to structural dynamics”. Springer Science & Business Media. http://dx.doi.org/10.1007/978-1-84996-323-7
Mendler, A., Döhler, M., & Ventura, C. E. (2022). “Sensor placement with optimal damage detectability for statistical damage detection”. Mechanical Systems and Signal Processing, 170, 108767. https://doi.org/10.1016/j.ymssp.2021.108767
Muthuraman, U., Hashita, M. S., Sakthieswaran, N., Suresh, P., Kumar, M. R., & Sivashanmugam, P. (2016). “An approach for damage identification and optimal sensor placement in structural health monitoring by genetic algorithm technique”. Circuits and Systems, 7(6), 814-823. http://dx.doi.org/10.4236/cs.2016.76070
Nguyen, Q. T., & Livaoğlu, R. (2022). ”Modal strain energy-based updating procedure for

damage detection: A numerical investigation". Journal of Mechanical Science and Technology, 36(4), 1709-1718. https://doi.org/10.1007/s12206-022-0307-3

Nouri Shirazi, M. R., Mollamahmoudi, H., & Seyedpoor, S. M. (2014). Structural damage identification using an adaptive multi-stage optimization method based on a modified particle swarm algorithm. Journal of Optimization Theory and Applications, 160(3), 1009-1019. https://doi.org/10.1007/s10957-013-0316-6

Ostachowicz, W., Soman, R., & Malinowski, P. (2019). "Optimization of sensor placement for structural health monitoring: A review". Structural Health Monitoring, 18(3), 963-988. https://doi.org/10.1177/14759217198256

Pastor, M., Binda, M., & Harčarik, T. (2012). "Modal assurance criterion". Procedia Engineering, 48, 543-548. https://doi.org/10.1016/j.proeng.2012.09.551

Peeters, B., & De Roeck, G. (2000), "Reference based stochastic subspace identification in civil engineering". Inverse problems in Engineering, 8(1), 47-74. https://doi.org/10.1080/174159700088027718

Rainieri, C., & Fabbrocino, G. (2014). "Operational modal analysis of civil engineering structures". Springer, New York, 142, 143. https://doi.org/10.1007/978-1-4939-0767-0

Rao, A., & Anandakumar, G. (2008). "Optimal sensor placement techniques for system identification and health monitoring of civil structures". Smart structures and systems, 4(4), 465-492. https://doi.org/10.12989/sss.2008.4.4.465

Ručevskis, S., Rogala, T., & Katunin, A. (2022), "Optimal sensor placement for modal-based health monitoring of a composite structure". Sensors, 22(10), 3867. https://doi.org/10.3390/s22103867

Sarparast Sadat, S., & Gholizad, A. (2026). A Robust Optimization of Sensor Placement for Truss Structures in Structural Health Monitoring. Iranian Journal of Science and Technology, Transactions of Civil Engineering, 1-17. https://doi.org/10.1007/s40996-026-02198-w

Simpkins, A. (2012). "System identification: Theory for the user", (ljung, l.; 1999)[on the shelf]. IEEE Robotics & Automation Magazine, 19(2), 95-96. https://doi.org/10.1109/MRA.2012.2192817

Teimouri, H., Davoodi, M. R., Mostafavian, S. A., & Khanmohammadi, L. (2021). Damage detection in double layer grids with modal strain energy method and Dempster-Shafer theory. Civil Engineering Infrastructures Journal, 54(2), 253-266. https://doi.org/10.22059/CEIJ.2020.294512.1644

Tong, K. H., Bakhary, N., Kueh, A. B. H., & Yassin, A. Y. (2014). "Optimal sensor placement for mode shapes using improved simulated annealing". Smart Struct. Syst, 13(3), 389-406. https://doi.org/10.12989/sss.2014.13.3.389

Ubertini, F., Gentile, C., & Materazzi, A. L. (2013). "Automated modal identification in operational conditions and its application to bridges". Engineering Structures, 46, 264-278. https://doi.org/10.1016/j.engstruct.2012.07.031

Zhan, J. Z., & Yu, L. (2014). An Effective Independence-Improved Modal Strain Energy Method for Optimal Sensor Placement of Bridge Structures. Applied Mechanics and Materials, 670, 1252-1255. https://doi.org/10.4028/www.scientific.net/AMM.670-671.1252

Yang, C. (2021). "An adaptive sensor placement algorithm for structural health monitoring based on multi-objective iterative optimization using weight factor updating". Mechanical Systems and Signal Processing, 151, 107363. https://doi.org/10.1016/j.ymssp.2020.107363